

## Greenland Ice Sheet Surface Temperature, Melt, and Mass Loss: 2000 – 2006

Dorothy K. Hall<sup>1</sup>, Richard S. Williams, Jr.<sup>2</sup>, Scott B. Luthcke<sup>3</sup>  
and  
Nicolo E. DiGirolamo<sup>4</sup>

<sup>1</sup>Cryospheric Sciences Branch, Code 614.1, NASA / Goddard Space Flight  
Center, Greenbelt, MD 20771

<sup>2</sup>U.S. Geological Survey, Woods Hole Science Center, Woods Hole, MA 02543

<sup>3</sup>Planetary Geodynamics Laboratory, Code 698, NASA / Goddard Space Flight  
Center, Greenbelt, MD 20771

<sup>4</sup>Science Systems and Applications, Inc.  
Lanham, MD 20706

### Popular Summary

Extensive melt on the Greenland Ice Sheet has been documented by a variety of ground and satellite measurements in recent years. If the well-documented warming continues in the Arctic, melting of the Greenland Ice Sheet will likely accelerate, contributing to sea-level rise. Modeling studies indicate that an annual or summer temperature rise of 1°C on the ice sheet will increase melt by 20-50% therefore, surface temperature is one of the most important ice-sheet parameters to study for analysis of changes in the mass balance of the ice-sheet.

The Greenland Ice Sheet contains enough water to produce a rise in eustatic sea level of up to 7.0 m if the ice were to melt completely. However, even small changes (centimeters) in sea level would cause important economic and societal consequences in the world's major coastal cities thus it is extremely important to monitor changes in the ice-sheet surface temperature and to ultimately quantify these changes in terms of amount of sea-level rise.

We have compiled a high-resolution, daily time series of surface temperature of the Greenland Ice Sheet, using the 1-km resolution, clear-sky land-surface temperature (LST) standard product from the Moderate-Resolution Imaging Spectroradiometer (MODIS), from 2000 – 2006. We also use Gravity Recovery and Climate Experiment (GRACE) data, averaged over 10-day periods, to measure change in mass of the ice sheet as it melt and snow accumulates. Surface temperature can be used to determine frequency of surface melt, timing of the start and the end of the melt season, and duration of melt. In conjunction with GRACE data, it can also be used to analyze timing of ice-sheet mass loss and gain.

We measured a +0.27°C a<sup>-1</sup> increase in mean, “clear-sky” surface temperature of the entire ice sheet, using MODIS LST data from 2001 through 2006 from mean-annual surface temperatures. (LST cannot be measured through cloudcover from MODIS.) All six major drainage basins show a trend toward higher mean surface temperature during the study period, and most show a trend toward a

---

longer melt season. However the northern basins show the greatest temperature increase during the study period, particularly during the winter months. While none of the observed trends is statistically significant in part due to the brevity of the record, they are consistent with trends seen using a variety of other observations.

Using both MODIS and GRACE data, the timing of mass loss (or gain) can be determined following initiation (or cessation) of surface melt. When <1% of the ice-sheet experienced surface melt, rapid (<15 days) and sustained mass loss below 2000-m elevation is triggered in 2004 and 2005 as recorded by GRACE. This result highlights the metastability of parts of the Greenland Ice Sheet and the vulnerability of the ice sheet to air-temperature increases. If air temperatures continue to rise over Greenland, increased surface melt will play a large role in ice-sheet mass loss.

## Greenland Ice Sheet Surface Temperature, Melt, and Mass Loss: 2000 – 2006

Dorothy K. Hall<sup>1</sup>, Richard S. Williams, Jr.<sup>2</sup>, Scott B. Luthcke<sup>3</sup>  
and  
Nicolo E. DiGirolamo<sup>4</sup>

<sup>1</sup>Cryospheric Sciences Branch, Code 614.1, NASA / Goddard Space Flight  
Center, Greenbelt, MD 20771

<sup>2</sup>U.S. Geological Survey, Woods Hole Science Center, Woods Hole, MA 02543

<sup>3</sup>Planetary Geodynamics Laboratory, Code 698, NASA / Goddard Space Flight  
Center, Greenbelt, MD 20771

<sup>4</sup>Science Systems and Applications, Inc.  
Lanham, MD 20706

### Abstract

A daily-time series of “clear-sky” surface temperature has been compiled of the Greenland Ice Sheet (GIS) using the 1-km resolution, clear-sky land-surface temperature (LST) standard-data product from the Moderate-Resolution Imaging Spectroradiometer (MODIS), from 2000 to 2006. Surface temperature is important because it is a sensitive indicator of surface-melt timing and duration. We also use the Gravity Recovery and Climate Experiment (GRACE) mass concentration, or mascon, solution data to study mass change on the GIS in relationship to surface melt from 2003 to 2006. The mean LST of the GIS increased during the last six years of the study period by  $\sim 0.27^{\circ}\text{C a}^{-1}$ . The LST increase was especially notable in the northern half of the ice sheet during the winter months and at higher elevations. Over the course of the study period, most of the six major drainage basins of the GIS experienced longer melt seasons, and a stable or later start and end of the melt season; however basins 4 and 5, in southern Greenland, showed dramatically earlier initiation of the melt season by up to 18 and 22 days, respectively. While none of the observed trends is statistically significant in part due to the brevity of the record, they are consistent with trends seen using a variety of other observations. We also show that when  $<1\%$  of the ice-sheet experienced surface melt, rapid ( $<15$  days) and sustained mass loss below 2000-m elevation is triggered in 2004 and 2005 as recorded by GRACE. Below 2000 m in 2004 and 2005, the ice sheet lost  $\sim 321$  and  $\sim 444$  Gt of mass, respectively, and experienced more melting in 2005 as compared to 2004. After cessation of surface melt (in 2003, 2004 and 2005), GRACE data show an increase in mass from accumulation, with a delay of  $<30$  days. The result that initiation of large-scale surface melt is followed rapidly by mass loss supports recent findings that surface meltwater is flowing rapidly to the base of the ice sheet causing acceleration of outlet glaciers. This result highlights the metastability of parts of the GIS and the vulnerability of the ice sheet to air-temperature increases. If air temperatures continue to rise over Greenland, increased surface melt will play a large role in ice-sheet mass loss.

## Introduction

The GIS contains enough water to produce a rise in eustatic sea level of  $\sim 7.0$  m if the ice were to melt completely (Gregory and others, 2004). Even small increases (centimeters) in sea level would cause important economic and societal consequences in the world's major coastal cities (Bindoff and others, 2007; Rowley and others, 2007). If the well-documented warming (ACIA, 2005; Richter-Menge and others, 2006; IPCC, 2007) continues in the Arctic, melting of the Greenland Ice Sheet (GIS) is likely to accelerate, augmenting the ongoing rise in sea level. Extensive melt and mass loss on the GIS has been documented in recent years (Krabill and others, 2000; Abdalati and Steffen, 2001; Joshi and others, 2001; Nghiem and others, 2001; Steffen and others, 2004; Steffen and Huff, 2005; Comiso, 2006a; Luthcke and others, 2006; Rignot and Kanagaratnam, 2006). Mass loss occurs through surface melting, percolation through the ice, and subglacier runoff, and when land-based ice calves into the sea. Meltwater that reaches the base of the ice-sheet lubricates the ice/bedrock interface increasing the velocity of outlet glaciers and thus accelerating mass loss (Zwally and others, 2002; Joughin and others, 2004; Rignot and Kanagaratnam, 2006; Steffen and others, 2006).

Model results indicate that an annual or summer temperature rise of  $1^{\circ}\text{C}$  on the GIS will increase ice melt by 20-50% (Oerlemans, 1991; Braithwaite and Olesen, 1993; Ohmura and others, 1996; Janssens and Huybrechts, 2000; Hanna and others, 2005). The surface temperature,  $T_s$ , of the GIS is influenced strongly by near-surface air temperature. Melting in areas that experience sustained increases in air temperature of  $\geq 0^{\circ}\text{C}$  and, where residual water content of the firn has been exceeded, will lead to a negative ice-sheet mass balance over large areas of the ice sheet if there is an excess of melt as compared to the previous winter's snowfall. Therefore, the  $T_s$  of the GIS is one of the most important ice-sheet parameters to study for forecasting changes in the mass balance of the ice-sheet.

Various satellite and airborne remote sensing and ground-based measurements may be used to assess the mass balance of the GIS. In this paper, however, we focus on clear-sky surface temperature, or land-surface temperature (LST) from 2000 through 2006, derived from the Moderate-Resolution Imaging Spectroradiometer (MODIS) flown on NASA's Terra satellite, and gravimetry data from the Gravity Recovery and Climate Experiment (GRACE) for the period from July 2003 through July 2006. Specifically, we: 1) analyze clear-sky LST and melt variability in each of the six major drainage basins of the GIS to look for patterns and short-term trends in  $T_s$  that may be relevant to observed changes in the Arctic; 2) calculate interannual melt-season timing and duration, and; 3) analyze the relationship between initiation and cessation of surface melt from MODIS LST data, and initiation and cessation of mass loss using GRACE gravimetry data.

## Background

Surface temperatures on the GIS have been studied on the ground using automatic weather station (AWS) data from the Greenland-Climatic Network (GC-Net) (Steffen and Box, 2001; Box, 2002) and from analysis of satellite sensor data (see for example, Key and Haeffliger, 1992; Haeffliger and others, 1993; Stroeve and Steffen, 1998; Shuman and others, 2001; Comiso and others, 2003; Comiso, 2006a). Using Advanced Very High Frequency Radiometer (AVHRR) weekly  $T_s$  maps at 6.25-km resolution from 1981 – 2005, Comiso (2006a) showed that warming predominates in the western Arctic, North America, Greenland, and much of Europe, while a cooling of the climate is observed elsewhere, such as in Russia. He also showed that the overall temperature trend poleward of 60°N is  $0.72 \pm 0.10^\circ\text{C}$  per decade, with an increase in surface temperature of the GIS of  $1.19 \pm 0.20^\circ\text{C}$  per decade, or an average of  $\sim 0.12^\circ\text{C a}^{-1}$ , between 1981 and 2005, with a possible 3+ day increase in the length of the melt season during the same period for the GIS. Recently, Hall and others (2006) showed the relationship between LST and ice-sheet mass balance using the 8-day composite, 5-km resolution MODIS LST product (MOD11C2) developed by Wan and others (2002). Mean LST of the GIS was shown to be highest in 2002 and 2005 in agreement with results of Steffen and Huff (2005) (<http://cires.colorado.edu/steffen/greenland/melt2005/>) who noted unusually-extensive melt of the ice sheet in 2002 and 2005 from analysis of passive and active microwave data. Similarly, years of relatively less surface melt, 2000 and 2001, were shown to have lower mean LSTs (Hall and others, 2006).

Although recent accelerated melting of the Arctic (Comiso 2006b) and the GIS has been measured (Abdalati and Steffen, 2001; Nghiem and others, 2001; Krabill and others, 2004; Rignot and Kanagaratnam, 2006; Chen and others, 2006; Velicogna and Wahr, 2006) and modeled (Box and others, 2006), longer-term warming has not shown a consistent trend. Hanna and Cappellen (2003) showed a significant cooling trend [ $-1.29^\circ\text{C}$  over a 44-year period (1958-2001)] for eight stations in coastal southern Greenland. Box (2002) showed spring and summer cooling in southern Greenland, a  $2 - 4^\circ\text{C}$  warming in western Greenland, and a possible  $1.1^\circ\text{C}$  warming at the ice-sheet summit for the period 1991 – 2000. And Steffen and others (2006) show a winter air temperature increase of up to  $0.5^\circ\text{C a}^{-1}$  over the last 15 years in the western GIS.

Much of the observed  $T_s$  variability on the GIS is linked to the North Atlantic Oscillation (NAO) (Appenzeller and others, 1998; Mote, 1998a, b; Huff and Steffen, 2006), sea ice extent, and large, explosive volcanic events (e.g., Mt. Pinatubo, Philippines, in June 1991) (Box, 2002). In particular, the NAO is highly correlated with surface-melt extent (Mote, 1998a).

The NAO is usually described as an oscillation (or “seesaw”) in the strength of the Icelandic Low and the Azores High. The Icelandic Low is a semi-permanent

center of low atmospheric pressure found over the Atlantic Ocean between Iceland and southern Greenland, as measured at Stykkishólmur, Iceland, and the Azores High is a semi-permanent high-pressure region found over the Atlantic Ocean at around 30°N latitude in winter [Ponta Delgada (Azores), Lisbon (Portugal), and Gibraltar have all been used as the southern station]. The positive NAO index phase shows a stronger-than-usual subtropical High and a deeper or stronger-than-usual Icelandic Low. The positive phase of the NAO is associated with an increased north – south pressure difference and results in more and stronger winter storms crossing the Atlantic Ocean on a more northerly track, and in colder and drier winters in Greenland (Hurrell, 1995; Rogers, 1997). The negative NAO index phase is characterized by a weak subtropical High and a weak Icelandic Low. The reduced pressure gradient results in fewer and weaker storms crossing on a more west-east path which permits milder winter temperatures in Greenland

[<http://www.atmosphere.mpg.de/enid/77d9810278d8243047762d9afac0ae3b,55a304092d09/193.html>]. The NAO is better characterized as an annular mode, and is increasingly being referred to (at least in the dynamical literature) as the Northern Annular Mode (NAM), or a north-south shift in atmospheric mass between the polar regions and the mid-latitudes, because it is not a true 'oscillation' (Thompson and others, 2003; Thompson, 2007). Thus in the remainder of this paper, we refer to the NAM instead of the NAO.

The correspondence between the rise in summer temperatures in coastal locations of the GIS, starting about 1995, and increased glacier activity suggests that warming has a nearly-immediate effect on the velocity of outlet glaciers, and that modest (1°C) increases in temperature can lead to large changes in the discharge of glacier ice to the ocean, most likely through the mechanism of transferring surface melt to the bed of the ice sheet through moulins and crevasses (Zwally and others, 2002). This is contrary to earlier hypotheses that an ice sheet may take tens or hundreds of years to respond to short-term air-temperature changes [see for example, Sugden and John (1976)].

Many studies have shown mass balance or melt characteristics in specific parts or basins of the GIS. Abdalati and Steffen (2001) show summer melt extent for different topographically-defined climate zones: a 21-year time series shows a positive melt trend of 1% a<sup>-1</sup>. Luthcke and others (2006) and Zwally and others (2005) reported the greatest mass loss in the southeastern part of the GIS. Rignot and Kanagaratnam (2006) show that the velocity of outlet glaciers has increased especially in the east-central, southern and western parts of the ice sheet, and is accompanied by accelerated retreat and thinning of the glacier termini and a corresponding increase in seismic activity related to the accelerated flow of outlet-glaciers (Ekström and others, 2006).

Luthcke and others (2006) found a significant mass loss of the GIS, using gravimetry data from the GRACE satellite, in the GIS in drainage basins 3 (east-central), 4 (southeast) and 6 (northwest), with basin 4 (southeast GIS)

dominating the mass loss for a two year period (2003-2005), and basins 1, 2 and 5 to be nearly in balance; they reported a mass gain of  $54 \text{ Gt a}^{-1}$   $>2000 \text{ m}$  and a loss of  $155 \text{ Gt a}^{-1}$  at elevations  $<2000 \text{ m}$ , with an overall net mass loss of the GIS from 2003 – 2005 of  $101 \pm 16 \text{ Gt a}^{-1}$ . Using aircraft laser and satellite radar altimetry, Krabill and others (2000 and 2004) and Zwally and others (2005) report a thinning of the GIS at elevations below approximately  $2000 \text{ m}$  around the margins and a thickening  $> \sim 2000 \text{ m}$ . Johannessen and others (2005) found an increase in surface elevation of the ice sheet above  $1500 \text{ m}$  of  $6.4 \pm 0.2 \text{ cm a}^{-1}$ . And Zwally and others (2005) concluded that the GIS is in approximate mass balance or perhaps has a slightly positive mass balance. Krabill and others (2004) documented an acceleration of mass loss from 1997–2003, when compared to the period ranging from 1993/4 to 1998/9, at elevations  $<2000 \text{ m}$ , and mass-balance equilibrium above  $\sim 2000 \text{ m}$ .

In summary, there appears to be a near-consensus from recent works that there is a small net mass loss of the GIS, with a general thinning at lower elevations (below  $\sim 2000 \text{ m}$ ) and a thickening at the higher elevations ( $>2000 \text{ m}$ ), with the southeastern parts of the ice sheet experiencing the greatest mass loss. This has been determined by analysis of data from sensors that record energy from different parts of the electromagnetic spectrum.

## Data and Methodology

For the present work, we use the 1-km pixel resolution MODIS LST standard daily product (MOD11A1), discussed in detail in Wan and others (2002), from Collection-4 reprocessing which provides surface temperatures over the Earth's land areas under clear-sky conditions. A cloud mask is generated from another MODIS standard product, MOD35 (Ackerman and others, 1998; Platnick and others, 2003), and is an input to the MOD11A1 LST algorithm.

For each day beginning 24 February 2000, through 31 December 2006, a 1-km resolution map of the LST of the GIS was compiled by digitally “mosaicking” MOD11A1 granules (or scenes) onto an Albers equal-area map of Greenland. (MODIS acquired its first image data on 24 February 2000 from the Terra satellite and has provided data nearly continually since then.)

Mean melt-season LST was calculated for the entire ice sheet, and within each of its six major drainage basins as defined by Zwally and others (2005) (Figure 1), during the period of most active surface melt, from 30 April / 1 May to 12 / 13 August (days 121 to 225) of each year (2000 – 2006). (Date varies depending on whether or not the year is a leap year.) We also computed mean-annual LST (2001 – 2006), and compared it with maps of mean-annual  $T_s$  from Steffen and Box (2001) and Cassano and others (2001).

To develop melt-frequency maps, we define “melt” as any pixel for which the LST was  $\geq 0^{\circ}\text{C}$ . We also calculated least-squares-fit lines for melt-season length, timing (start and end) and duration in each of the six major drainage basins of the GIS for the 7-year study period, 2000 – 2006. We define the beginning of the melt season as the first two days of consecutive melt, and the end of the melt season as the last two days of consecutive melt. For example, if days 1 and 3 experience melt and day 2 is cloudy, there are two days of consecutive melt according to our definition.  $T_s$  is usually higher under cloudcover than under clear skies because of strong radiational cooling from the snow/ice surface under clear skies that does not occur when skies are cloudy. Thus, the assumption is that the LST will remain at  $0^{\circ}\text{C}$  (or above – see Limitations and Uncertainties section for a discussion of this) on the cloudy days between the days with melt as determined from the LST data.

We also compared the melt onset and duration with GRACE local mass-concentration, or mascon, data, to study the relationship of surface melt to ice-sheet mass loss. GRACE denotes the twin satellites launched in March 2002 that are flying in formation about 220-km apart; changes in the distance between the satellites are used to make detailed measurements of the Earth's gravity field enabling mass-change studies of the GIS that result from precipitation (mass gain) and ablation or iceberg calving (mass loss). The lead satellite, for example, will be pulled away farther from the trailing satellite when it passes above an area of larger mass concentration. The resolution is fine enough to permit basin-by-basin studies of the GIS using  $\sim 10$ -day averages of mascon data (Luthcke and others, 2006). Before mass loss can be estimated from the GRACE data, mascon solutions must be corrected for other geophysical signals. In this work, the 3-year trend as well as Earth and ocean tide and atmospheric mass signals have been removed. See Luthcke and others (2006) for details about the GRACE mascon data.

## Results

**Mean Melt-Season LST.** The mean LST map for the 7-year study period during the most-active part of the melt season, May through mid-August, is provided in Figure 2. The digital elevation model (DEM) of Bamber and others (2001) was overlaid, and the 2000 and 3000 m contours are shown (62.2% of the ice sheet lies above 2000 m). During the most-active part of the melt season, the mean LST of the GIS for the study period is  $-9.64 \pm 6.34^{\circ}\text{C}$ , varying from a low of  $-11.03 \pm 6.59^{\circ}\text{C}$  in 2000, to a high of  $-8.82 \pm 6.24^{\circ}\text{C}$  in 2002 (Table 1). Note that in Figure 2 the margins of the southern part of the GIS (mean-melt-season LST) are only a few degrees above  $0^{\circ}\text{C}$  (also see Box, 2002; and Hanna and Cappelen, 2003). Thus those areas are particularly vulnerable to rapid mass loss with further increase in  $T_s$ .



Mean LST during the most-active part of the melt season was also calculated in each of the six major drainage basins. The years 2000 and 2001 experienced the lowest mean LST in all of the basins, followed by 2006. The years 2002 and 2005 experienced the highest mean LST in most of the basins (Table 1). Fausto and others (2007) noted a lot of variation in melting of the GIS between years, and particularly strong melting in 2002, 2003 and 2005. There is a trend toward higher mean, melt – season LST in each of the drainage basins during the study period that it is strongest in basins 1, 2 and 6, the northern basins, with basins 1 and 2 having the most-pronounced positive slopes ( $0.274^{\circ}\text{C a}^{-1}$  and  $m = 0.311^{\circ}\text{C a}^{-1}$ , respectively) (Figure 3) though the trend lines are not statistically significant. Basin 4 has the highest mean LST, and the least interannual variability in mean LST (lowest standard deviation) of all the basins because of the preponderance of pixels at  $0^{\circ}\text{C}$  compared to the other basins where the range in LST is relatively greater. This is not surprising, because drainage basin 4 is a relatively small basin and has the most marine exposure.

**Mean-Annual and Seasonal LST.** We calculated the mean-annual LST in two different ways. First, we took the average of all the LSTs of each pixel from 1 January 2001 through 31 December 2006, giving equal weight to each LST value [Figure 4 (left image)]. Then we averaged all the LSTs available for each month, determined a monthly-mean LST, and from the monthly data we calculated a mean-annual LST [Figure 4 (right image)]. We then compared our maps with a map of mean-annual  $T_s$  derived by Steffen and Box (2001) from modeling and analysis of AWS data, and a map of mean-annual temperature derived using the Polar MM5 model by Cassano and others (2001).

There is a warm bias to the mean-annual LST map shown in Figure 4 (left image). This occurs mainly because of missing days in the winter months due to cloud masking problems (see discussion in Limitations and Uncertainties section). As compared to the maps of mean-annual  $T_s$  of Steffen and Box (2001) and Cassano and others (2001), our MODIS-derived mean-annual LSTs are up to  $\sim 10^{\circ}\text{C}$  higher at the highest elevations, when we give equal weight to each LST in calculating the mean LST (Figure 4 [left image]). However if we calculate mean-annual LST by first calculating monthly averages, as shown in Figure 4 (right image), results are much closer to those of Steffen and Box (2001) and Cassano and others (2001), with temperatures at the highest elevations being up to  $\sim 5^{\circ}\text{C}$  higher. Both LST maps in Figures 4 show closer agreement with the Steffen and Box (2001) and Cassano and others (2001) maps at the lowest elevations of the ice sheet. It is clear that the accuracy of the LST-derived maps is reduced because of the inability to measure LST through cloudcover, especially during the wintertime, however that may not fully explain the higher LSTs that we find. The  $T_s$  has increased since the Steffen and Box (2001) and Cassano and others (2001) maps were produced (see Steffen and others, 2005), and it is therefore difficult to say how closely the maps “should” match especially at the higher elevations, where enhanced warming has been measured using the LST data.

The year 2001 experienced the lowest mean-annual LST when all pixel values were given equal weight to calculate the mean-annual LST (Table 2). As we saw with the data from the active-melt period, there is a trend in all basins toward higher mean-annual LST during the study period, but the trend is stronger with the mean-annual LST data (Figure 5). The most-pronounced positive slopes characterize the northern basins: 1 ( $m=0.377^{\circ}\text{C a}^{-1}$ ), 2 ( $m=0.446^{\circ}\text{C a}^{-1}$ ) and 6 ( $m=0.383^{\circ}\text{C a}^{-1}$ ), and the least-positive characterizes Basin 4 ( $m=0.004^{\circ}\text{C a}^{-1}$ ) as was also noted for the most-active part of the melt season. However, in part due to the brevity of the record (6 years), none of these trends is statistically significant.

During the six-year period from January 2001 through December 2006, there is an overall increase in mean LST of the entire ice sheet of  $\sim 0.27^{\circ}\text{C a}^{-1}$ , with the higher-elevation areas ( $>2000\text{ m}$ ) contributing more toward the observed increased mean-annual temperatures (Figure 6).

Seasonal plots were also produced using each pixel to develop a mean-seasonal LST for each year from 2000 – 2006 (Figure 7). The winter of 2000 could not be used due to the lack of MODIS data for January and most of February 2000. The increase in LST is greatest during the winter season, where the slope ( $m=0.890^{\circ}\text{C a}^{-1}$ ) is the highest of the four seasons, and the mean-annual LSTs are more variable than they are in other seasons.

***Melt-season Timing, Duration, and Frequency of Melt.*** Melt-season length was studied in each of the six major drainage basins (Figure 8). Most of the basins (1, 2, 4 and 5) show a slightly longer melt season over the course of the study period, and a later start and end of the melt season (see positive slopes in Basins 1, 2 and 6, and a later start only in basin 3). However basins 4 and 5, in the southern half of the GIS, each show a pronounced trend toward an earlier start and end of the melt season, with the more pronounced trend being toward an earlier start of the melt season in both basins 4 and 5 by up to  $\sim 18$  and  $22$  days, respectively. It is the earlier start of the melt season that is the main factor causing an overall longer melt season during the study period in these basins. Not only are the trends shown in Figure 8 not statistically significant, but they are likely to be quite different as more years are added to these plots.

The frequency of melt, especially in the southern half of the GIS (see basins 4 and 5) increases beginning in 2002, especially for very short-term melt of 1 – 2 day duration (Figure 9). The lowest frequency of melt is observed in 2000, and this is consistent with the mean melt-season LST of the GIS being the lowest that year (Table 1).

The number of years with a melt season (at least 2 days of consecutive melt to begin and end the melt season) from 2000 – 2006 is shown in Figure 10. Comparing Figures 9 and 10, note that large areas of the northeastern (in year

2002) and southern GIS (in years 2003, 2004, 2005 and 2006) show short-term melt of generally seven days or less (see purple color on map), the importance of which is discussed in the Discussion and Conclusions section.

**Mass Change.** We now focus on melt on the GIS at elevations <2000 m using MODIS LST and mascon solution data from GRACE. Shortly after surface melt begins (defined herein as 1% of the ice sheet experiencing melt) rapid mass loss occurs in the years 2004 and 2005, the only years during which reprocessed GRACE mascon data are complete (Figure 11). Initiation of mass loss appears to be very sensitive to small amounts of surface melt. We calculated a melt index (MI) anytime the percentage of clear-sky pixels for the entire ice sheet experiencing melt was 1% or greater according to the LST maps. The MI is the sum of the daily percentages of melt over a specified period of time. In the 2004 and 2005 melt seasons, the MI is 1046.50 and 1115.20, respectively, and there is a corresponding greater mass loss in 2005 (443.7 Gt) as compared to 2004 (321.1 Gt). There was a <15-day delay from melt onset ( $MI \geq 1$ ) to initiation of mass loss in both 2004 and 2005. There is a longer delay from cessation of melt to the beginning of sustained mass gain (<30 days) for 2003, 2004 and 2005. This is reasonable because there can be a significant amount of liquid water in the upper layers of snow and firn of the ice sheet even after the ice sheet surface refreezes. Since the mascon data represent ~10-day averages, the exact number of days of delay from onset of melt to initiation of mass loss cannot be calculated.

The annual contribution of glacial meltwater from the GIS to changes in eustatic sea level can be estimated by dividing the annual mass loss in (Gt) by 400, the volume of ice, in cubic km, needed to raise (or lower) global sea level by 1 mm (Williams and Hall, 1993). Thus for the 2004 and 2005 melt seasons discussed above, the total contribution to sea-level rise (SLR) was 1.9 mm, according to the mascon data for those parts of the ice <2000 m. This was partly compensated for by mass gains during the accumulation seasons at all elevations.

**NAM Forcing.** Is there a relationship between the NAM and the observation of wintertime temperature increases in the northern basins of the GIS during the MODIS era? The NAM has shown a trend toward a high index polarity during the last few decades, especially during the Northern Hemisphere winter, with a relaxation in the past decade (Cohen and Barlow, 2005). Though a relaxation, or weakening, of the NAM has been associated with warmer temperatures on the GIS, there are simply not enough years in the data record to attribute the recent relaxation in the NAM index to the observed 6 – 7-year increase in the surface temperatures of the GIS reported herein. It is also interesting to note that climate models have failed to simulate a consistent trend in the NAM in response to increasing greenhouse gases (IPCC, 2007; Thompson, 2007).

## Limitations and Uncertainties

Although the measurement accuracy of MOD11A1 is  $\pm 2^{\circ}\text{C}$  over ice-and-snow surfaces in the absence of cloud (Wan and others, 2002; Hall and others, 2006), the major limitation in the derived LST occurs when thin clouds are not detected by the cloud mask that is used in the MOD11A1 algorithm. Under such conditions an LST is calculated for the pixel, but the derived value may not be accurate. Depending on the type and altitude of the thin cloud, and the  $T_s$  of the ice/snow, the derived LST may be higher or lower than the actual  $T_s$ .

Over ice, it is more difficult to discriminate clear sky from clouds during the polar night with MODIS data due, in part, to a small or lack of thermal contrast between the cloud and the ice/snow surface, and temperature inversions that may occur over the ice sheet. Thus the number of total pixels available to compile the LST maps varies by season, with a much lower number of pixels available for use during the winter as compared to the summer (Table 3). Therefore the mean LST values do not represent actual mean values of  $T_s$  which is why they are called “clear-sky” surface temperatures. An average of only 26.0 days is available to retrieve LST during the winter seasons (January through March) during the six-year study period, while almost 2.5 times as many days - an average of 64.7 days - is available during the summer seasons (June through August) (Table 3).

To calculate mean-annual LST, all MODIS LST values from the ice sheet were used (that is, all cloud-free pixels) that passed the quality-assurance tests in the algorithm. A total of 1,910,905 1-km pixels covers the GIS, but in any given day, fewer than that number of pixels is available to develop an LST map. Thus, calculation of mean LST results in using different numbers of total pixels for different areas in different years. [Note: the area of the inland ice (GIS) was estimated at 1,736,095  $\text{km}^2$  by Weidick (1995); our measurement of the ice-sheet area is within 10% of that number. The difference is caused by the inclusion of nunataks and other ice-free areas and possible differences in the land masks used.]

A few spurious pixels ( $>0^{\circ}\text{C}$ ) are found on the ice sheet, and for the purpose of the calculations of mean LST, these pixel values were changed to  $0^{\circ}\text{C}$ . For instance, for March through November 2006, out of 285,924,066 total clear-sky pixels studied, only 0.02% were  $>2^{\circ}\text{C}$ . Incorrect cloud masking by the MODIS cloud mask is the most likely reason that a few pixels provide erroneous LSTs. Other possible, but less likely reasons for these elevated LST values include the possibility that LST in a pixel that contains many melt ponds could exceed  $0^{\circ}\text{C}$  sometime during the melt season, and, because of mixed-pixel effects (ice and melt ponds) could cause a pixel value to exceed the freezing point of water. If the water temperature is  $>0^{\circ}\text{C}$  and the ice temperature is  $0^{\circ}\text{C}$ , then a mixed pixel could have a temperature  $>0^{\circ}\text{C}$ .

Compared to earlier work by Hall and others (2006), who used 5-km MODIS 8-day composite LST data, the daily, 1-km resolution MODIS maps used in the present study provide improved results. There is a difference in the way that the LST is calculated to derive the 5- and 1-km LST products. A split-window algorithm is used to generate the 1-km maps, and a day-night difference algorithm is used to generate the 5-km maps (Wan and others, 2002). Thus both the difference in algorithms and the difference in temporal and spatial resolution would contribute to different LSTs over the same general area of the ice sheet. For instance, in the most-active part of the melt season, mean LST values of the GIS are consistently lower, by  $\sim 0.5 - 1.0^{\circ}\text{C}$ , using the higher-resolution data. The lower LSTs reported herein using the 1-km daily data are more consistent with the published mean-annual  $T_s$  map of Steffen and Box (2001) and Cassano and others (2001).

MODIS Collection 5 (C5) data production began in January 2007, and should be completed by September 2008. The primary difference between Collections 4 and 5, relative to this work, is improved cloud masking in Collection 5, especially during nighttime conditions which will result in a more accurate and less-conservative cloud mask. Therefore more clear-sky pixels should be available to calculate LST, and this is expected to improve the accuracy in producing maps of LST, especially in the winter months.

## Discussion and Conclusions

We have calculated least-squares-fit or trend lines for the LST data of the entire ice sheet, and in each of the major drainage basins (Figures 3 – 8). While none of the trends is statistically significant in part due to the brevity of the record, they are consistent with trends seen using a variety of other observations, and are therefore of interest to report. However each additional point (year) can quite easily change the “trend” since there are so few years of data available. Additionally, as noted earlier, and also by Fausto and others (2007), the interannual variability in surface melt is quite high. Thus it may take many more years to develop a consistent picture of the GIS melt and LST patterns and to make a determination about external forcings and statistically-significant trends.

***Melt-Season, Seasonal, and Mean-Annual LSTs.*** Our results show relatively-low mean LSTs in 2000, 2001 and 2006, and relatively-high mean LSTs in 2002 and 2005 (Table 1), during the period of most-active melt. These results agree with those of Steffen and others (2006) who found enhanced melting in 2002 and 2005 using passive-microwave data, and Fausto and others (2007) who found greater melt in 2002 and 2005 using MODIS data. Comparison of our mean-annual LST map [Figure 4 (left image)] with the mean-annual  $T_s$  maps of Steffen and Box (2001) and Cassano and others (2001) shows that the MODIS-derived LSTs are higher (by up to  $\sim 10^{\circ}\text{C}$  at the highest elevations) than these published values of mean-annual  $T_s$  which have some ground validation. This is mainly

due to a limitation of the LST algorithm, which has overly-conservative cloud masking during the wintertime, thus biasing the mean-annual LST data to higher temperatures when all pixels are given equal weight to calculate the mean-annual LST. When the mean-annual LST [Figure 4 (right image)] map is calculated by deriving monthly averages before calculating the mean-annual LST, the values are closer to the published values of Steffen and Box (2001) and Cassano and others (2001), but still show higher LSTs, especially at the highest elevations of the ice sheet. Because of ice-sheet warming, especially in recent years at the higher elevations ( $>2000$  m), it is difficult to say how closely either of the maps shown in Figure 4 compares to the actual mean  $T_s$  of the ice sheet.

Slopes of least-squares-fit lines of MODIS-derived LST vary at different elevations, and in different drainage basins of the GIS during the study period. Each of the six major drainage basins of the GIS reacts differently because of its unique topographic and geographic position and relationship to internal and external forcings. Thus each has different mean LSTs and differences in melt-season length, duration, and timing.

Meteorological-station data from land-based stations that are associated with drainage basin 4 show trends toward increasing air temperature. Temperature records at Angmagssalik station in southeastern Greenland ( $65^{\circ}40'N$ ,  $37^{\circ}20'W$ ) show a  $3^{\circ}C$  increase in annual air temperature from approximately the early 1980s to the present (Rignot and Kanagaratnam, 2006). Across the Denmark Strait, about 700 km to the east of Angmagssalik, data from the meteorological station at Stykkishólmur, northwestern Iceland ( $65^{\circ}2'N$ ,  $22^{\circ}40'W$ ), show dramatically-increased summer-mean temperatures in recent years (Jónsson and Garðarsson, 2001; Hanna and others, 2004; Oddur Sigurðsson, written communication, 2007), and increasing mean-annual temperatures. The increased melt observed in basin 4 is consistent with the meteorological-station data showing higher air temperatures in recent years.

Though not statistically significant, the increase we found in mean-annual LST ( $0.27^{\circ}C\ a^{-1}$ ) represents a trend toward increasing  $T_s$  and is comparable to, though greater than, the rate of increase of mean  $T_s$  of the GIS from 1981 – 2005 given by Comiso (2006a) ( $\sim 0.12^{\circ}C\ a^{-1}$ ) of  $T_s$  based on monthly AVHRR data at 6.25-km resolution, and the  $0.11^{\circ}C\ a^{-1}$  increase in temperature at the summit of the ice sheet found by Box (2002). The trend toward an increase in mean-annual LST is driven by the LST increase at the higher elevations ( $>2000$  m) as seen in Figure 6. Comiso (2006b) noted an increase in the rate of temperature increase in parts of the Arctic in recent years, so the greater rate of temperature increase, as compared to the Comiso (2006a) and Box (2002) results, seems reasonable.

The observed temperature increases in the northern basins of the GIS (Figures 3 and 5) are driven by the enhanced seasonal warming during the wintertime seen in Figure 7 and as discussed by Box (2002) and Steffen and others (2005). Steffen and others (2006) report that winter air temperatures in the western GIS

increased by as much as  $0.5^{\circ}\text{C a}^{-1}$  during the past 15 years, and our MODIS LST results show an increase in LST of  $\sim 0.33^{\circ}\text{C a}^{-1}$  from 2001 to 2006 (Figure 6). The LST increases are greater during the winter than during spring, summer and fall (Figure 7). The trends are not statistically significant and the enhanced warming in the northern basins during wintertime may not continue.

***Melt-Season Timing and Duration.*** Interannual differences in melt-season timing have changed quite rapidly in southeastern and southwestern Greenland, especially in basins 4 and 5, during the last seven years. The melt season began up to 18 and 22 days earlier in basins 4 and 5, respectively, from 2000 to 2006. However most of the other basins experienced no real change, or a later start of the melt season during the study period, except for basin 6 which showed a more-pronounced later start (and end) of the melt season over the course of the study period. We also found trends toward an increase in the length of the melt season in most of the basins, and especially in basin 5 (Figure 8). Basin 4, and the southern and western parts of basin 5, are especially vulnerable to rapid melt because the mean  $T_s$  is already near  $0^{\circ}\text{C}$  according to the Steffen and Box (2001) and Cassano and others (2001) maps of  $T_s$ , and our melt-season LST map (Figure 2).

Basins 4 and 5 are also the basins with the highest mean LSTs, the greatest amount of melt during the most-active part of the melt seasons, and where most of the accelerated outlet-glacier activity is occurring. Most of the increase in velocity of outlet glaciers (Joughin and others, 2004; Rignot and Kanagaratnam, 2006; Ekström and others, 2006) is occurring in basins 4 and 5 where a large volume of short-term ( $\leq 7$  days) surface meltwater is produced (Figures 9 and 10). Especially notable is the observation by Ekström and others (2006) that, out of the 136 seismic events that they studied (1993 – 2005), relating to increase in velocity of outlet-glaciers, 93 (or 68%) occurred in basin 4 in southeast Greenland.

***Relationship of Surface Melt to Mass Loss.*** The sensitivity of the initiation of mass loss to surface melt is striking in the 2004 and 2005 melt seasons, with  $<1\%$  of ice-sheet melt needed to trigger mass loss. GRACE gravimetry data show general mass loss of the GIS since its 2003 launch (Luthcke and others, 2006; Velicogna and Wahr, 2006). When surface melt begins, mass loss is initiated within  $<15$  days thereafter as seen in Figure 11 for the 2004 and 2005 melt seasons. The dramatic influence of the surface melt on mass loss has been demonstrated, but not previously on such a large scale over the entire ice sheet.

There are two possible mechanisms for surface melt contributing to rapid mass loss. One possibility is that evaporation may increase substantially when surface melt begins, especially in windy parts of the ice sheet. Another possibility, as discussed in Zwally and others (2002), is that surface melt can flow rapidly to the base of the ice sheet causing enhanced lubrication at the ice/rock interface and thus cause faster movement of outlet glaciers and accelerated mass loss. This is

thought (Rignot and Kanagaratnam, 2006; Howat and others, 2007) to be responsible for rapid acceleration of outlet glaciers, and thus increased mass loss.

Gravimetry mascon data from the GRACE satellite are limited in length, but as more years of MODIS and GRACE data become available, it will be interesting to see if the relationship between surface melt and mass loss holds. Similar studies at the basin scale will also be conducted in the future.

**Importance of Surface Melt.** Even short-term melt ( $\leq 7$  days) observed over large parts of the southern part of the ice sheet in 2003 through 2006 (Figure 9) is important for the temperature regime of the GIS. Echelmeyer and others (1992) show that latent-heat release upon refreezing just above the equilibrium line is a major source of warming in snow and firn. Surface meltwater may infiltrate 3 m or more into the cold firn where it may refreeze and thus not run off, causing densification and compaction of the firn (Benson, 1962 and 1996; Echelmeyer and others, 1992). This can lower the surface elevation, whereas lower temperatures raise the surface elevation according to Zwally and others (2005) who require surface temperature as a parameter in the firn-compaction model. Accurate surface temperatures, derived from satellite, are necessary to provide accurate surface-elevation measurements using satellite-laser altimetry, such as topographic profiles produced by the Ice, Cloud, and land Elevation (ICESat) Satellite.

**External Forcings.** Though the NAM has weakened (positive and negative index values are generally less pronounced) in recent years, as compared to the late 1990s and early 2000, there are not enough years of data to determine a statistically-significant NAM trend that would explain the pattern of LST increase that we have observed (enhanced LST increases in the northern basins during the wintertime).

**Conclusion.** LST data provide melt-season extent, length, timing and duration. In combination with GRACE gravimetry data, the influence of surface melt on the initiation and cessation of mass loss may be assessed. This key relationship between surface melt and initiation of mass loss points strongly to rapid movement of surface water to the base of the ice sheet. It also highlights the extreme vulnerability of the ice sheet to increasing air temperatures, especially in the southern half of the ice sheet where melt-season temperatures are only a few degrees from 0°C. If air temperatures continue to rise over Greenland, increased surface melt will play a large role in ice-sheet mass loss.



## **Acknowledgments**

The authors would like to thank Jay Zwally of / NASA / Goddard Space Flight Center for providing us with the Greenland Ice Sheet drainage basin data; Koni Steffen / CIRES / University of Colorado for providing us with the Steffen and Box (2001) surface-temperature map; Jonathan Bamber / Bristol Glaciology Centre, University of Bristol, UK, for providing us with the DEM of Greenland; and Dave Thompson / Colorado State University for discussions about the Northern Annular Mode. We also thank Oddur Sigurðsson / National Energy Authority, Iceland, for data from the Stykkishólmur meteorological station, and an associated discussion. We thank Joey Comiso / NASA / Goddard Space Flight Center, Ted Scambos of the National Snow and Ice Data Center, and two anonymous reviewers for their reviews. This work was supported by NASA's Cryospheric Sciences Program.

## References

- Abdalati, W. and K. Steffen. 2001. Greenland ice sheet melt extent: 1979-1999. *Journal of Geophysical Research*, 106(D24):33,983-33,989.
- ACIA, 2005. Arctic Climate Impact Assessment. Cambridge, U.K. Cambridge University Press, 1042 p.
- Ackerman, S.A., K.I. Strabala, P.W. Menzel, R.A. Frey, C.C. Moeller and L.E. Gumley. 1998. Discriminating clear sky from clouds with MODIS. *Journal of Geophysical Research*, 103(D24):32,141-32,157.
- Appenzeller, C., J. Schwander, S. Sommer and T.F. Stocker. 1998. The North Atlantic Oscillation and its imprint on precipitation and ice accumulation in Greenland. *GRL*, 25(11):1939-1942.
- Bamber, J.L., S. Ekholm and W.B. Krabill. 2001. A new, high-resolution digital elevation model of Greenland fully validated with airborne laser altimeter data. *Journal of Geophysical Research*, 106(B4):6733-6745, 2001.
- Benson, C.S. 1962 & 1996. Stratigraphic studies in the snow and firn of the Greenland ice sheet, Snow, Ice and Permafrost Research Establishment (now U.S. Army Cold Regions Research and Engineering Laboratory), Research Report 70 (reprinted and updated in 1996), 93 p. + appendices.
- Bindoff, N.L., J. Willebrand, V. Artale, A. Cazenave, J. Gregory, S. Gulev, K. Hanawa, C. Le Quéré, S. Levitus, Y. Nojiri, C.K. Shum, L.D. Talley and A. Unnikrishnan. 2007. Observations: oceanic climate change and sea level, in Solomon, S., D. Qin, M. Manning, Z. Chen, M. Marquis, K.B. Averyt, M. Tignor and H.L. Miller (eds.), *Climate change 2007: the physical basis*, Contribution of Working Group 1 to the Fourth Assessment Report of the Intergovernmental Panel on Climate Change: Cambridge, U.K., Cambridge University Press, pp. 384-432. [<http://ipcc-wg1.ucar.edu/wg1/wg1-report.html>]
- Box, J.E. 2002. Survey of Greenland instrumental temperature records: 1873 – 2001. *International Journal of Climatology*, 22(15):1829-1847.
- Box, J.E., D.H. Bromwich, B.A. Veenhuis, L.-S. Bai, J.C. Stroeve, J.C. Rogers, K.Steffen, T. Haran and S.H. Wang. 2006. Greenland Ice Sheet surface mass balance variability (1988 – 2004) from calibrated polar MM5 output. *Journal of Climate*, 19:2783-2800.
- Braithwaite, R.J., and O.B. Olesen. 1993. Seasonal variation of ice ablation at the margin of the Greenland ice sheet and its sensitivity to climate change, Qamanârssûp sermia, West Greenland. *Journal of Glaciology*, 39(132):267-274.
- Cassano, J.J., J.E. Box, D.H. Bromwich, L. Li and K. Steffen. 2001. Evaluation of polar MM5 simulations of Greenland's atmospheric circulation. *Journal of Geophysical Research*, 106(D4):33,867-33,889.
- Chen, J.L., C.R. Wilson and B.D. Tapley. 2006. Satellite gravity measurements confirm accelerated melting of Greenland ice sheet. *Science*, 313:1958-1960.
- Cohen, J. and M. Barlow. 2005. The NAO, the AO, and Global Warming: how closely related? *Journal of Climate*, 18(21):4498-4513.

- Comiso, J., J. Yang, S. Honjo and R.A. Krishfield. 2003. Detection of change in the Arctic using satellite and in situ data. *Journal of Geophysical Research*, 108(C12):3384, doi:10.1029/2002JC001347.
- Comiso, J.C. 2006a. Arctic warming signals from satellite observations. *Weather*, 61(3):70-76.
- Comiso, J.C. 2006b. Abrupt decline in the Arctic winter sea ice cover. *GRL*, 33, L18504, doi:10.1029/2006GL 027341, 2006.
- Echelmeyer, K., W.D. Harrison, T.S. Clarke and C. Benson. 1992. Surficial glaciology of Jakobshavns Isbrae, West Greenland: Part II. Ablation, accumulation and temperature. *Journal of Glaciology*, 38(128):169-181.
- Ekström, G., M. Nettles and V.C. Tsai. 2006. Seasonality and increasing frequency of Greenland glacial earthquakes. *Science*, 311:1756-1758.
- Fausto, R.S., C. Mayer and A.P. Ahlstrøm. 2007. Satellite-derived surface type and melt area of the Greenland ice sheet using MODIS data from 2000 to 2005, *Annals of Glaciology*, 46:35-42.
- Gregory, J.M., P. Huybrechts and S.C.B. Raper. 2004. Threatened loss of the Greenland ice sheet. *Nature*, 428:616 (8 April 2004).
- Hall, D.K., R.S. Williams, Jr., K.A. Casey, N.E. DiGirolamo and Z. Wan. 2006. Satellite-derived, melt-season surface temperature of the Greenland Ice Sheet (2000-2005) and its relationship to mass balance. *GRL*, 33:L11501, doi:10.1029/2006GL026444.
- Hanna, E., J. Cappelen. 2003. Recent cooling in coastal southern Greenland and relation with the North Atlantic Oscillation. *GRL*, 30(3):doi10.1029/2002GL015797.
- Hanna, E., T.Jónsson, J.E.Box. 2004. An analysis of Icelandic climate since the nineteenth century. *International Journal of Climatology*, 24(10):1193-2004.
- Hanna, E., P. Huybrechts, I. Janssens, J. Cappelen, K. Steffen and A. Stephens. 2005. Runoff and mass balance of the Greenland ice sheet: 1958-2003. *Journal of Geophysical Research*, 110(D13108):doi10.1029/2004JD005641.
- Haefliger, M., K. Steffen and C. Fowler. 1993. AVHRR surface temperature and narrow-band albedo comparison with ground measurements for the Greenland ice sheet. *Annals of Glaciology*, 17:49-54.
- Howat, I.M., I.R. Joughin and T.A. Scambos. 2007. Rapid changes in ice discharge from Greenland outlet glaciers. *Science*, 315(5818):1559-1561.
- Huff, R. and K. Steffen. 2006. Large scale atmospheric circulation and melt variability on the Greenland Ice Sheet. *Eos Transactions AGU*, 87(52), Fall Mtg. Suppl.
- Hurrell, J.W. 1995. Decadal trends in the North Atlantic oscillation: regional temperatures and precipitation. *Science*, 269(5224):676-679.
- IPCC, 2007. Summary for Policymakers, in Solomon, S., D. Quin, M. Manning, Z. Chen, M. Marquis, K.B. Averyt, M. Tignor and H.L. Miller (eds.), *Climate change 2007: The physical basis*, Contribution of Working Group 1 to the Fourth Assessment Report of the Intergovernmental Panel on Climate Change: Cambridge, U.K., Cambridge University Press, pp. 1-18. [<http://ipcc-wg1.ucar.edu/wg1/wg1-report.html>]

- Janssens, I., and P. Huybrechts. 2000. The treatment of meltwater retention in mass-balance parameterizations of the Greenland ice sheet. *Annals of Glaciology*, 31:133-140.
- Johannessen, O.M., K. Khvorostovsky, M.W. Miles and L.P. Bobylev. 2005. Recent ice-sheet growth in the interior of Greenland. *Science*, 310:1013-1016.
- Jónsson, T. and H. Garðarsson. 2001. Early Instrumental Meteorological Observations in Iceland. *Climatic Change*, 48(1):169-187.
- Joshi, M., C.J. Merry, K.C. Jezek and J.F. Bolzan. 2001. An edge detection technique to estimate melt duration, season and melt extent on the Greenland ice sheet using passive microwave data. *GRL*, 28(15):3497-3500.
- Joughin, I., W. Abdalati and M. Fahnestock. 2004. Large fluctuations in speed on Greenland's Jakobshavn Isbrae glacier. *Nature*, 432:608.
- Key, J. and M. Haefliger. 1992. Arctic ice surface temperature retrieval from AVHRR thermal channels. *Journal of Geophysical Research*, 97(D5):5885-5893.
- Krabill, W., W. Abdalati, E. Frederick, S. Manizade, C. Martin, J. Sontag, R. Swift, R. Thomas, W. Wright and J. Yungel. 2000. Greenland ice sheet: High-elevation balance and peripheral thinning. *Science*, 289:428-430.
- Krabill, W., E. Hanna, P. Huybrechts, W. Abdalati, J. Cappelen, B. Csatho, E. Frederick, S. Manizade, C. Martin, J. Sonntag, R. Swift, R. Thomas, W. and J. Yungel. 2004. Greenland Ice Sheet: Increased coastal thinning, *GRL*, 31, L24402, doi:10.1029/2004GL021533.
- Luthcke, S.B., H.J. Zwally, W. Abdalati, D.D. Rowlands, R.D. Ray, R.S. Nerem, F.G. Lemoine, J.J. McCarthy and D.S. Chinn. 2006. Recent Greenland ice mass loss by drainage system from satellite gravity observations. *Science*, 19 October 2006, 314(5803):1286-1289.
- Mote, T. 1998a. Mid-tropospheric circulation and surface melt on the Greenland ice sheet. Part I: atmospheric teleconnections. *International Journal of Climatology*, 18(2):111-130.
- Mote, T. 1998b. Mid-tropospheric circulation and surface melt on the Greenland ice sheet. Part II: synoptic climatology. *International Journal of Climatology*, 18(2):131-145.
- Nghiem, S., K. Steffen, R. Kwok and W.-Y. Tsai. 2001. Detection of snowmelt regions on the Greenland ice sheet using diurnal backscatter change. *Journal of Glaciology*, 47(159):593-547.
- Oerlemans, J. 1991. The mass balance of the Greenland Ice Sheet: sensitivity to climate change as revealed by energy-balance modeling. *Holocene*, 1:40-49.
- Ohmura, A., M. Wild and L. Bengtsson. 1996. A possible change in mass balance of the Greenland and Antarctic ice sheets in the coming century. *Journal of Climate*, 9:2124-2135.
- Platnick S., M.D. King, S.A. Ackerman, W.P. Menzel, B.A. Baum, J.C. Riédi, R.A. Frey. 2003. The MODIS cloud products: algorithms and examples from Terra. *IEEE Transactions on Geoscience and Remote Sensing*, 41(2):459-473.
- Richter-Menge, J. and 24 others. 2006. State of the Arctic Report. NOAA OAR Special Report, NOAA/OAR/PMEL, Contribution No. 2952 from NOAA, Pacific Marine Environmental Laboratory, Seattle, WA, 36 p.

- Rignot, E. and P. Kanagaratnam. 2006. Changes in the velocity structure of the Greenland Ice Sheet. *Science*, 311:986-990.
- Rogers, J.C. 1997. North Atlantic storm track variability and its association to the North Atlantic Oscillation and climate variability of northern Europe. *Journal of Climate*, 10(7):1635-1647.
- Rowley, R.J., J.C. Kostelnick, D. Braaten, X. Li and J. Meisel, 2007. Risk of rising sea level to population and land areas. EOS (Transactions of the American Geophysical Union), 88(9):105 & 107.
- Shuman, C.A., K. Steffen, J.E. Box and C.R. Stearns. 2001. A dozen years of temperature observations at the Summit: central Greenland automatic weather stations 1987-99. *Journal of Applied Meteorology*, 40:741-752.
- Steffen, K. and J. Box. 2001. Surface climatology of the Greenland ice sheet: Greenland climate network 1995-1999. *Journal of Geophysical Research*, 106(D24):33,951-33,964.
- Steffen, K., S.V. Nghiem, R. Huff, and G. Neumann. 2004. The melt anomaly of 2002 on the Greenland Ice Sheet from active and passive microwave satellite observations. *GRL*, 31, L20402, doi:10.1029/2004GL020444.
- Steffen, K., N. Cullen and R. Huff. 2005. Climate variability and trends along the western slope of the Greenland Ice Sheet during 1991–2004. *Proceedings of the 85<sup>th</sup> Annual American Meteorological Society Annual Meeting*, San Diego, Ca., Session J4.4.
- Steffen, K., H.J. Zwally, J.A. Rial, A. Behr and R. Huff, 2006. Climate variability, melt-flow acceleration, and ice quakes at the western slope of the Greenland Ice Sheet. *Eos Transactions AGU*, 87(52), Fall Mtg. Suppl.
- Steffen, K. and R. Huff website:  
<http://cires.colorado.edu/science/groups/steffen/greenland/melt2005/>.
- Stroeve, J. and K. Steffen. 1998. Variability of AVHRR-derived clear-sky surface temperature over the Greenland ice sheet. *Journal of Applied Meteorology*, 37:23-31.
- Sugden, D.E. and B.S. John, 1976. Glaciers and Landscape. A Geomorphological Approach. John Wiley & Sons, New York, 376 p.
- Thomas, R., B. Csatho, C. Davis, C. Kim, W. Krabill, S. Manizade, J. McConnell and J. Sonntag. 2001. Mass balance of higher-elevation parts of the Greenland ice sheet. *Journal of Geophysical Research*, 106(D24):33,707-33,716.
- Thompson, D.W.J., S. Lee and M.P. Baldwin. 2003. Atmospheric processes governing the Northern Hemisphere Annular Mode/North Atlantic Oscillation. *In AGU Geophysical Monograph 134, The North Atlantic Oscillation – Climatic Significance and Environmental Impact*, J.W. Hurrell, Y. Kushnir, M. Visbeck and G. Ottersen (eds.), pp. 81-112.
- Thompson, D.W.J., 2007. A brief introduction to the annular modes and annular mode research. <http://horizon.atmos.colostate.edu/ao/introduction.html> (March 17, 2007).
- Velicogna, I. and J. Wahr. 2006. Acceleration of Greenland ice mass loss in spring 2004. *Nature*, 443(21):329-331doi:10.1038/nature05168.

- Wan, Z., Y. Zhang, Q. Zhang, and Z.-L. Li. 2002. Validation of the land-surface temperature products retrieved from Terra Moderate Resolution Imaging Spectroradiometer data. *Remote Sensing of Environment*, 83:163-180.
- Wiedick, A. 1995. Greenland, with a section on Landsat images of Greenland by Williams, R.S., Jr. and J.G. Ferrigno. Satellite Image Atlas of Glaciers of the World (R.S. Williams, Jr. and J.G. Ferrigno (eds.): U.S. Geological Survey Professional Paper 1386-C, 141 p.
- Williams, R.S., Jr. and D.K. Hall. 1993. *Glaciers*; in Gurney, R.J., J.L. Foster and C.L. Parkinson, eds. Atlas of Earth Observations Related to Global Change. Cambridge, U.K., Cambridge University Press, pp.401-422.
- Zwally, H.J., W. Abdalati, T. Herring, K. Larsen, J. Saba, and K. Steffen. 2002. Surface melt-induced acceleration of Greenland ice-sheet flow. *Science*, 297(5579):218-222.
- Zwally, H.J., M.B. Giovinetto, J. Li, H.G. Cornejo, M.A. Beckley, A.C. Brenner, J.L. Saba and D. Yi. 2005. Mass changes of the Greenland and Antarctic ice sheets and shelves and contributions to sea-level rise: 1992 – 2002. *Journal of Glaciology*, 51(175):509-527.

## Tables

Table 1. Mean and standard deviation LSTs, in °C, of the six major drainage basins of the Greenland Ice Sheet for the most-active part of the melt season, May through mid-August, 2000 – 2006. The mean and standard deviation for the entire ice sheet (all) are also given.

Table 2. Mean and standard deviation LSTs, in °C, of the six major drainage basins of the Greenland Ice Sheet for January through December, 2001 – 2006. The mean and standard deviation for the entire ice sheet (all) are also given. Because the month of January and most of February 2000 were unavailable (the MODIS sensor first began acquiring data on 24 February 2000), the year 2000 is not included.

Table 3. Percent of total possible LST observations (pixels) per season. Note the reduced percentage of observations in the winter and fall as compared to spring and summer.

Table 1. Mean and standard deviation land-surface temperature, LSTs, in °C, of the six major drainage basins of the Greenland Ice Sheet for the most-active part of the melt seasons, May through mid-August, 2000 – 2006. The mean and standard deviation for the entire ice sheet (all) are also given.

Basin	2000	2001	2002	2003	2004	2005	2006	All Years
1	-11.68±6.56	-12.07±6.69	-8.97±6.19	-9.33±6.44	-10.03±5.37	-8.77±6.31	-10.97±5.42	-10.13±6.24
2	-13.35±6.55	-12.90±6.30	-9.73±6.85	-10.64±6.46	-11.00±6.27	-10.30±6.52	-11.75±5.74	-11.28±6.50
3	-10.70 ±6.23	-10.48±5.98	-8.74±6.14	-9.24±5.94	-9.20±6.09	-8.91±6.16	-9.72±5.64	-9.55±6.07
4	-6.77±5.31	-6.50±5.18	-6.09±5.04	-5.91±5.07	-5.88±5.48	-5.96±5.49	-6.19±5.14	-6.18±5.26
5	-9.64±6.16	-8.64±6.15	-7.93±5.63	-7.67±6.03	-7.88±6.14	-7.87±5.99	-8.62±5.81	-8.29±6.02
6	-12.00±6.59	-11.52±6.71	-9.81±6.17	-10.34±6.43	-10.60±5.96	-9.38±6.29	-10.82±5.78	-10.58±6.32
All	-11.03±6.59	-10.62±6.56	-8.82±6.24	-9.08±6.33	-9.42±6.16	-8.83±6.31	-10.03±5.87	-9.64±6.34



Table 2. Mean and standard deviation land-surface temperature, LSTs, in °C, of the six major drainage basins of the Greenland Ice Sheet for January through December, 2001 – 2006. The mean and standard deviation for the entire ice sheet (all) are also given. Because the month of January and most of February 2000 were unavailable (the MODIS sensor first began acquiring data on 24 February 2000), the year 2000 is not included.

Basin	2001	2002	2003	2004	2005	2006	All Years
1	-21.03±11.28	-18.44±11.75	-19.84±12.09	-18.55±11.05	-18.28±11.14	-18.75±10.28	-19.13±11.33
2	-21.35±10.74	-18.97±11.73	-20.09±11.68	-18.80±10.84	-18.52±10.58	-18.75±10.24	-19.40±11.05
3	-18.10±10.00	-17.06±10.88	-17.46±11.23	-17.34±10.62	-16.66±9.97	-16.83±9.91	-17.23±10.46
4	-14.11±9.67	-14.32±10.02	-13.70±10.47	-14.46±10.39	-14.18±9.71	-14.01±9.85	-14.12±10.03
5	-16.36±10.18	-15.87±10.43	-15.86±10.88	-16.00±10.65	-15.56±10.01	-15.93±10.07	-15.93±10.39
6	-19.69±10.90	-18.12±10.93	-19.60±11.23	-18.57±10.65	-17.36±10.53	-17.68±10.14	-18.52±10.78
All	-18.72±10.79	-17.42±11.17	-18.07±11.54	-17.45±10.83	-16.96±10.47	-17.20±10.22	-17.63±10.87

Table 3. Percent of total possible LST observations (pixels) per season.  
 Note the reduced percentage of observations in the winter and fall as compared to spring and summer.

Year	winter	spring	summer	fall
2000	--	62.45	53.64	37.99
2001	25.15	50.37	66.91	42.17
2002	15.90	59.74	66.70	49.05
2003	30.95	65.52	66.84	46.41
2004	29.45	67.89	68.47	36.57
2005	26.49	64.75	63.54	37.59
2006	28.01	61.66	66.61	36.10

## Figures

Figure 1. Six major drainage basins of the Greenland Ice Sheet (GIS) as modified from Zwally and others (2005). A land mask (shown in green) is included that was not part of the Zwally and others map. Ice caps and other glaciers that lie outside the margins of the GIS are shown in grey within the land mask. Only the Zwally and others major drainage basins and not the sub-basins delineated by Zwally and others are shown.

Figure 2. Map showing mean land-surface temperature, LST, of the Greenland Ice Sheet for the most-active part of the melt season (days 121 – 225) during the study period (2000 – 2006) as determined from MODIS LST data products (Wan and others, 2002). The 2000- and 3000-m contour lines from the Bamber and others (2001) digital-elevation model are shown. A land mask is shown in green.

Figure 3. Plot showing mean land-surface temperature, LST, in each of six major drainage basins of the Greenland Ice Sheet for the most-active part of the melt season (days 121 – 225) of each year, 2000 – 2006, as determined from MODIS LST data products (Wan and others, 2002).

Figure 4. Left - map showing mean-annual land-surface temperature, LST, of the Greenland Ice Sheet calculated using a technique that gives equal weight to all pixels in the calculation of the mean-annual LST. Right – map showing mean-annual LST calculated using monthly average LST to calculate mean-annual LST. The 2000- and 3000-m contour lines from the Bamber and others (2001) digital-elevation model are shown. A land mask is shown in green.

Figure 5. Plots showing mean-annual land-surface temperature, LST, in each of six major drainage basins for each year, 2001 – 2006, as determined from MODIS LST data products (Wan and others, 2002). The year 2000 is excluded because MODIS data from January and most of February are not available.

Figure 6. Mean-annual land-surface temperatures, LSTs, for the entire ice sheet, showing mean-annual LST over the study period at two different elevation ranges: 2000 m and below, and >2000 m, as determined from the Bamber and others (2001) digital-elevation model. The lower solid line represents the higher elevation range (lower LSTs), and the upper solid line represents the lower elevation range (higher LSTs). The dotted lines are the error bars.

Figure 7. Mean-seasonal land-surface temperatures, LSTs, for the entire ice sheet. Note the greater increase in mean-winter LST over the course of the study period as compared to the other seasons.

Figure 8. Timing and duration of melt seasons, 2000 – 2006, in each of the six major drainage basins of the Greenland Ice Sheet as determined from MODIS land-surface temperature, LST, data products developed by Wan and others (2002). The “melt season” is based on two consecutive days of melt to begin

and end the melt season; see text for further explanation. The formula for the slope of the trend line for the start of the melt season (see solid line) is shown in the bottom in the figure, and the formula for the slope of the trend line for the end of the melt season (see dashed line) is shown at the top in the figure. Duration of the melt season is shown with the vertical bars; least-squares fit lines are fitted to the points.

Figure 9. Number of days of melt on the Greenland Ice Sheet, 29 February / 1 March to 29 / 30 November (days 60 – 334) of each year, 2000 – 2006 based on MODIS land-surface temperature data products (Wan and others, 2002). Black lines delineate the six major drainage basins. A land mask is shown in green.

Figure 10. Number of years with a melt season on the Greenland Ice Sheet as discussed in the text. Black lines delineate the six major drainage basins. A land mask is shown in green.

Figure 11. MODIS-derived percent of melt (see text for explanation) with Gravity Recovery and Climate Experiment (GRACE)-derived mass concentration (mascon) data, in Gt, for the entire Greenland Ice Sheet, for July 2003 through July 2006. The mascon plot is shown with the 3-year trend, as well as Earth and ocean tide and atmospheric mass signals removed.

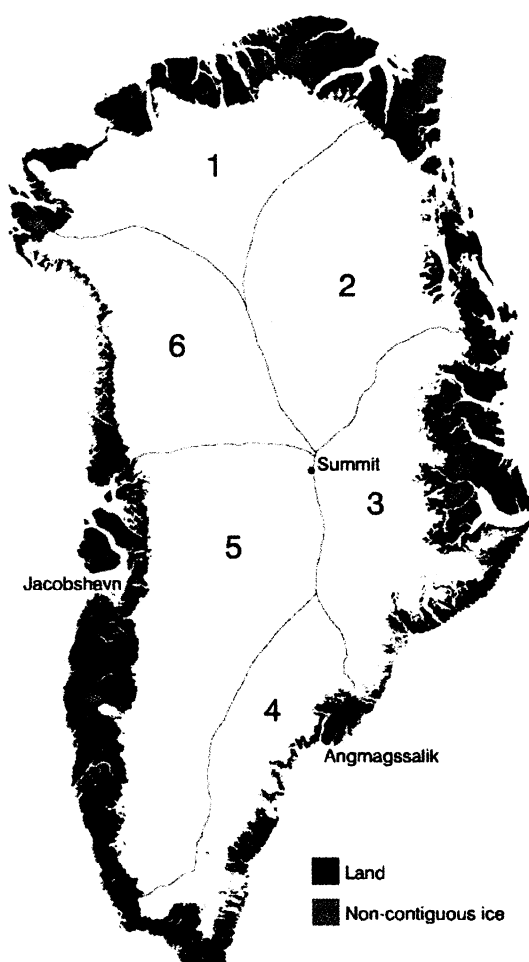


Figure 1. Six major drainage basins of the Greenland Ice Sheet (GIS) as modified from Zwally and others (2005). A land mask (shown in green) is included that was not part of the Zwally and others map. Ice caps and other glaciers that lie outside the margins of the GIS are shown in grey within the land mask. Only the Zwally and others major drainage basins and not the sub-basins delineated by Zwally and others are shown.



Figure 2. Map showing mean land-surface temperature, LST, of the Greenland Ice Sheet for the most-active part of the melt season (days 121 – 225) during the study period (2000 – 2006) as determined from MODIS LST data products (Wan and others, 2002). The 2000- and 3000-m contour lines from the Bamber and others (2001) digital-elevation model are shown. A land mask is shown in green.

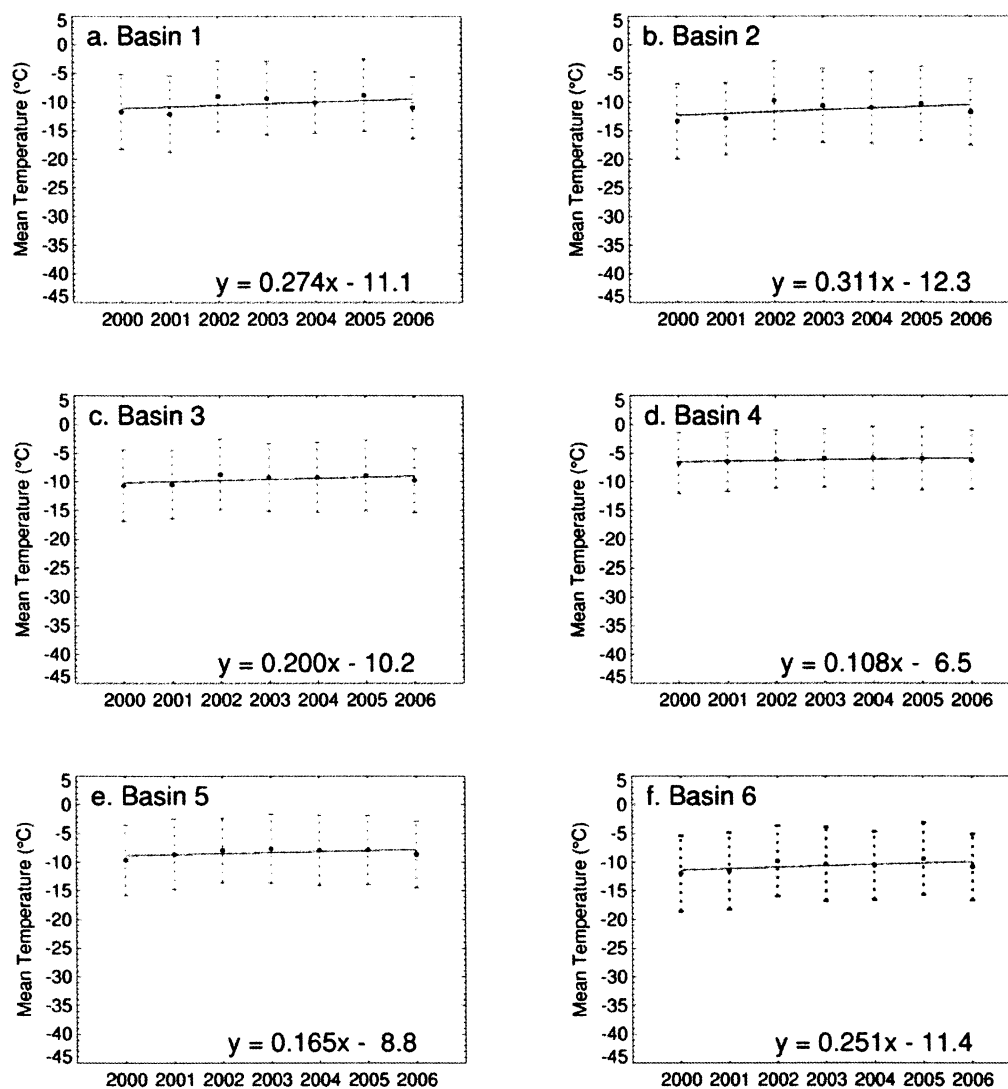


Figure 3. Plot showing mean land-surface temperature, LST, in each of six major drainage basins of the Greenland Ice Sheet for the most-active part of the melt season (days 121 – 225) of each year, 2000 – 2006, as determined from MODIS LST data products (Wan and others, 2002).



Figure 4. Left - map showing mean-annual land-surface temperature, LST, of the Greenland Ice Sheet calculated using a technique that gives equal weight to all pixels in the calculation of the mean-annual LST. Right - map showing mean-annual LST calculated using monthly average LST to calculate mean-annual LST. The 2000- and 3000-m contour lines from the Bamber and others (2001) digital-elevation model are shown. A land mask is shown in green.



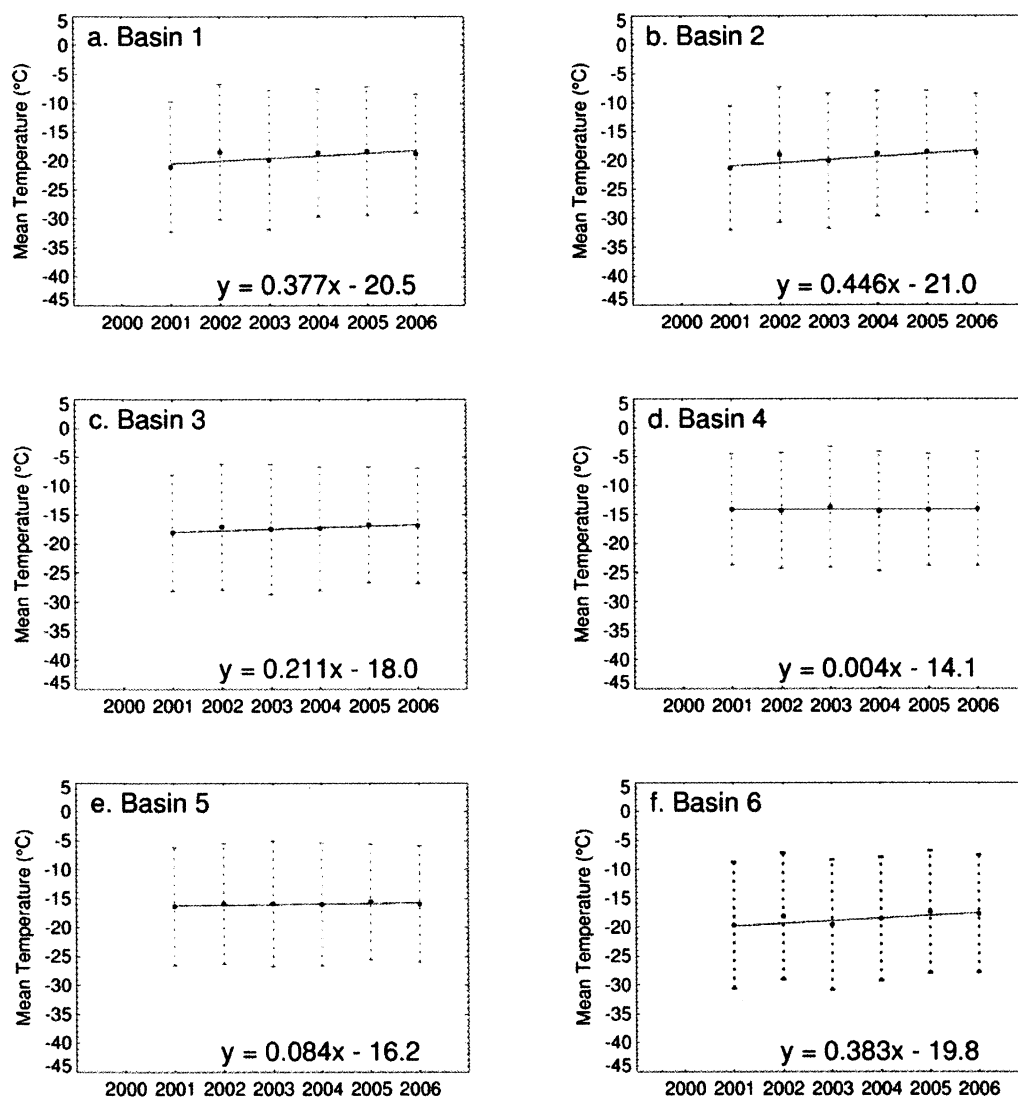


Figure 5. Plots showing mean-annual land-surface temperature, LST, in each of six major drainage basins for each year, 2001 – 2006, as determined from MODIS LST data products (Wan and others, 2002). The year 2000 is excluded because MODIS data from January and most of February are not available.

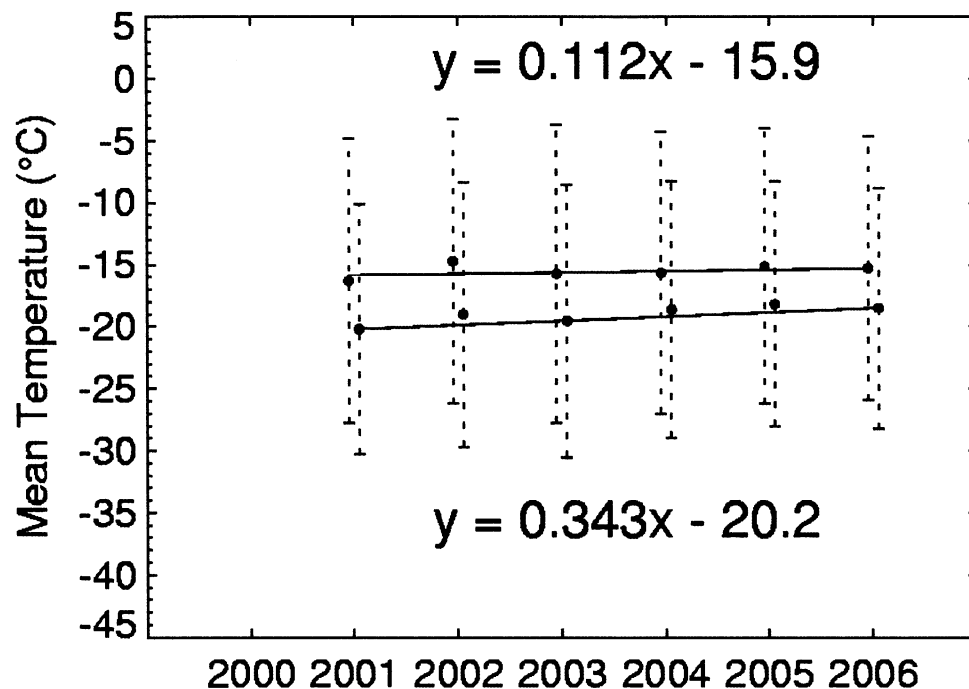


Figure 6. Mean-annual land-surface temperatures, LSTs, for the entire ice sheet, showing mean-annual LST over the study period at two different elevation ranges: 2000 m and below, and >2000 m, as determined from the Bamber and others (2001) digital-elevation model. The lower solid line represents the higher elevation range (lower LSTs), and the upper solid line represents the lower elevation range (higher LSTs). The dotted lines are the error bars.

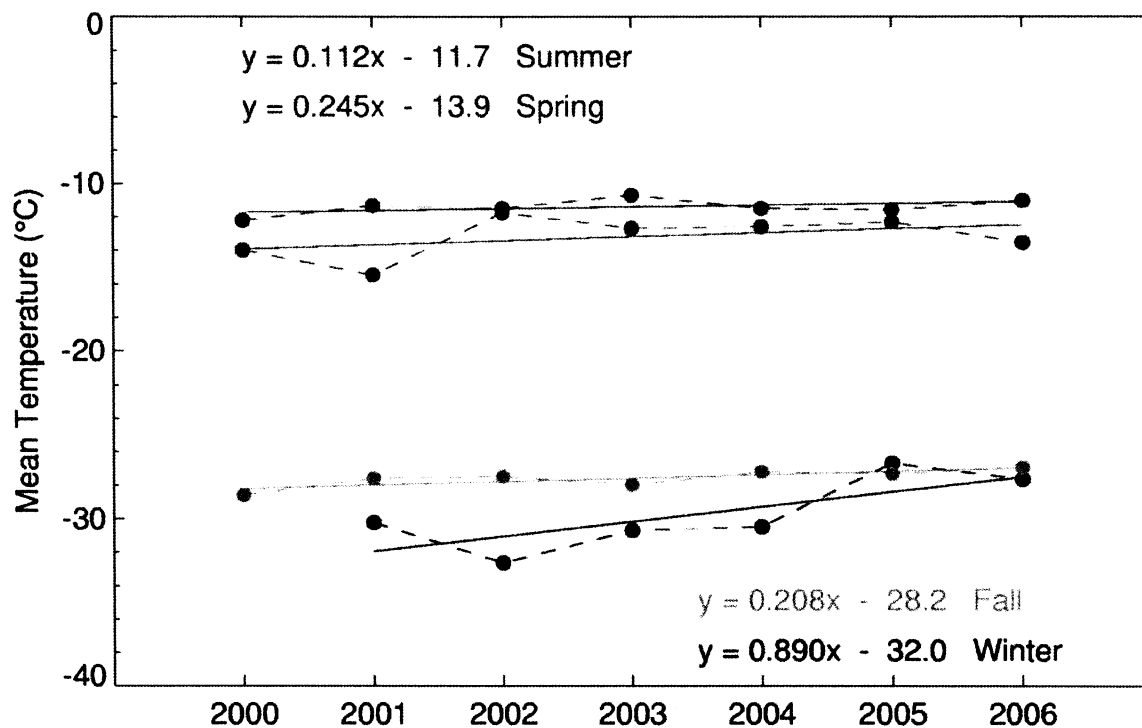


Figure 7. Mean-seasonal land-surface temperatures, LSTs, for the entire ice sheet. Note the greater increase in mean-winter LST over the course of the study period as compared to the other seasons.

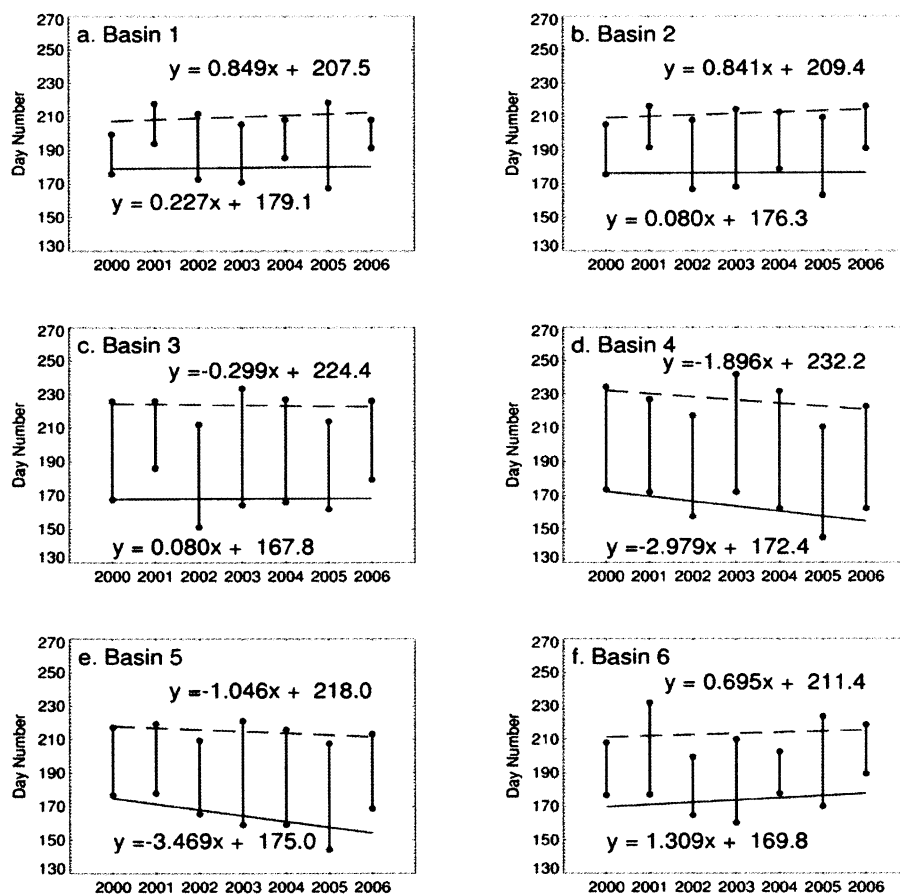


Figure 8. Timing and duration of melt seasons, 2000 – 2006, in each of the six major drainage basins of the Greenland Ice Sheet as determined from MODIS land-surface temperature, LST, data products developed by Wan and others (2002). The “melt season” is based on two consecutive days of melt to begin and end the melt season; see text for further explanation. The formula for the slope of the trend line for the start of the melt season (see solid line) is shown in the bottom in the figure, and the formula for the slope of the trend line for the end of the melt season (see dashed line) is shown at the top in the figure. Duration of the melt season is shown with the vertical bars; least-squares fit lines are fitted to the points.

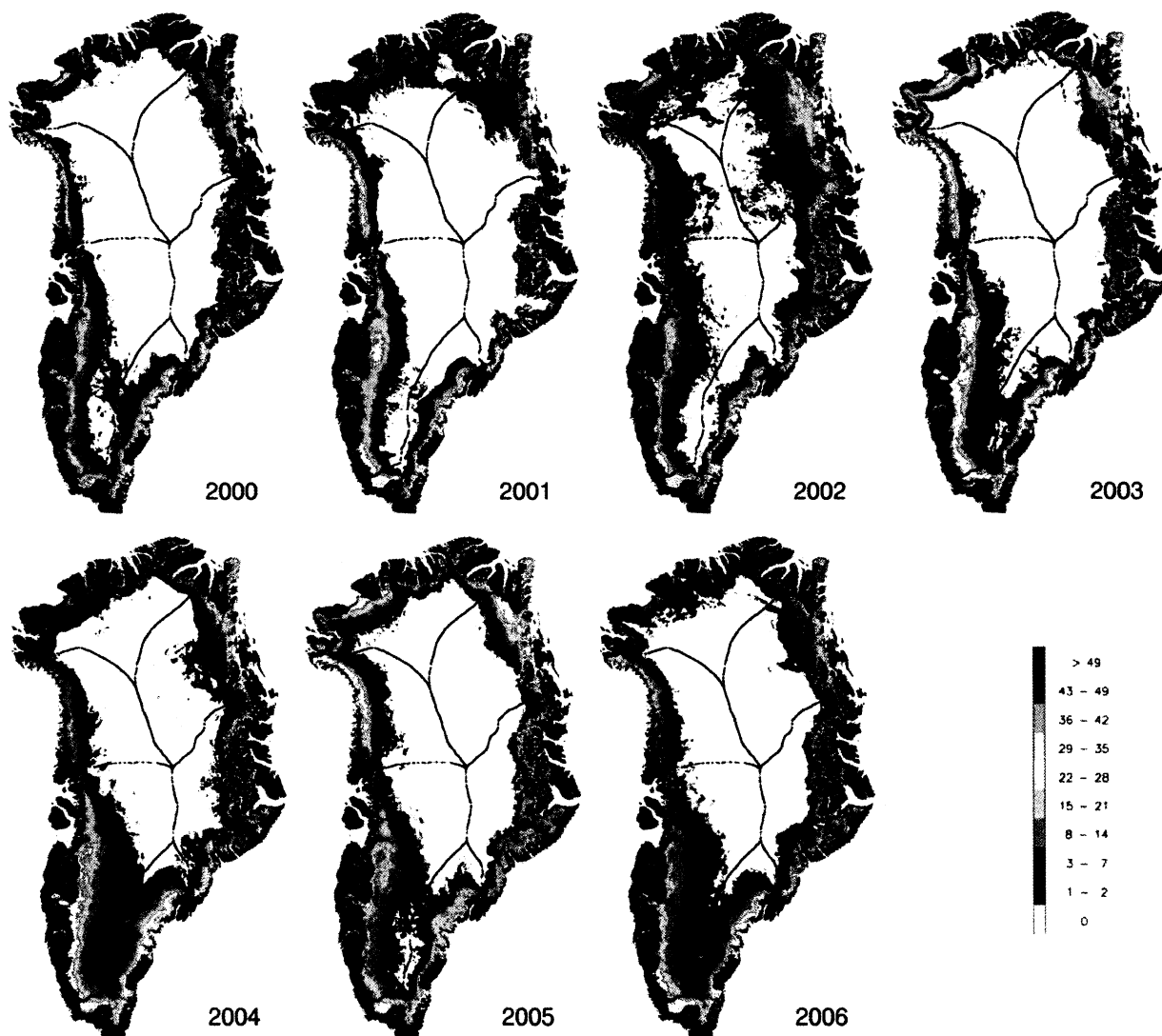


Figure 9. Number of days of melt on the Greenland Ice Sheet, 29 February / 1 March to 29 / 30 November (days 60 – 334) of each year, 2000 – 2006 based on MODIS land-surface temperature data products (Wan and others, 2002). Black lines delineate the six major drainage basins. A land mask is shown in green.

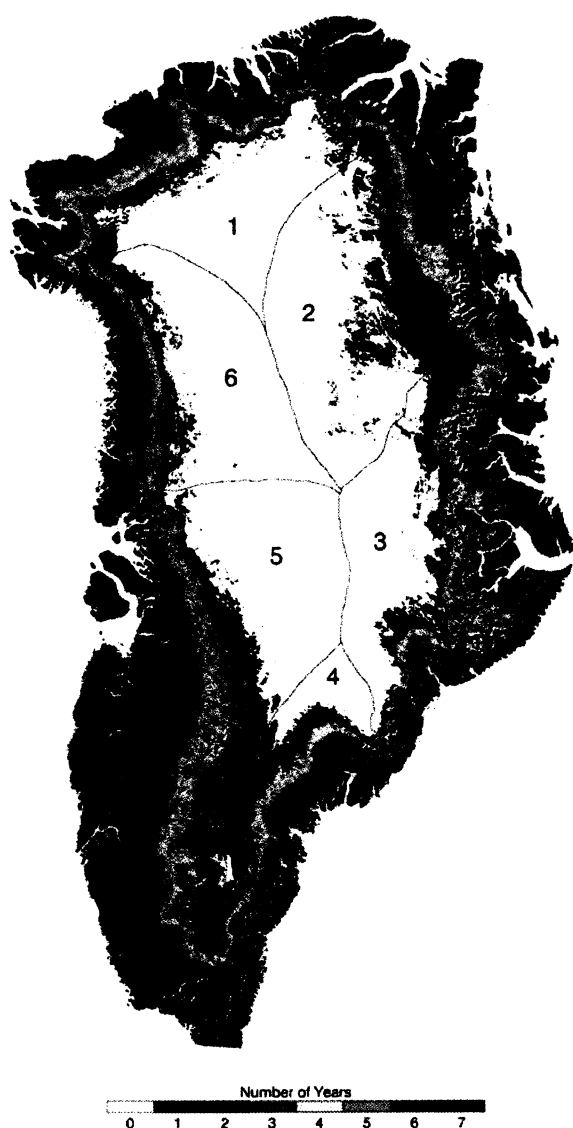


Figure 10. Number of years with a melt season on the Greenland Ice Sheet as discussed in the text. Black lines delineate the six major drainage basins. A land mask is shown in green.

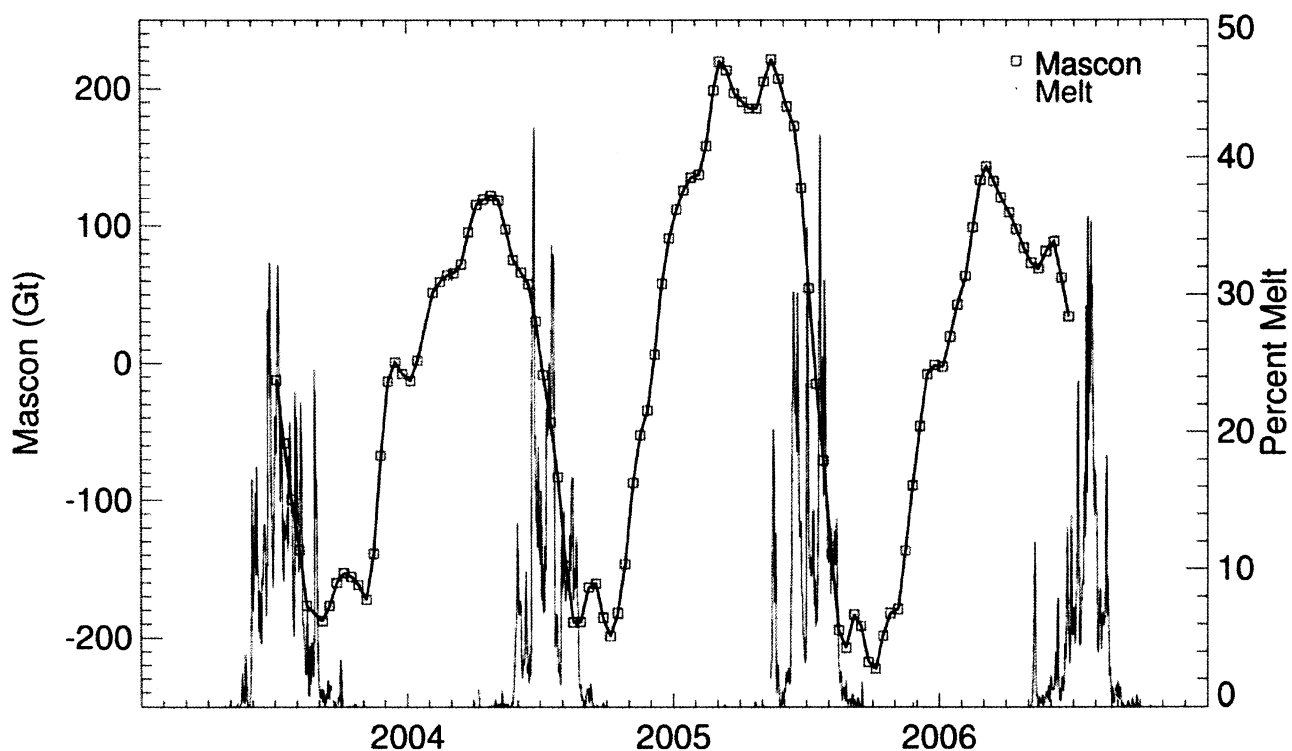


Figure 11. MODIS-derived percent of melt (see text for explanation) with Gravity Recovery and Climate Experiment (GRACE)-derived mass concentration (mascon) data, in Gt, for the entire Greenland Ice Sheet, for July 2003 through July 2006. The mascon plot is shown with the 3-year trend, as well as Earth and ocean tide and atmospheric mass signals removed.